

## The Study of Floating Nuclear Power Plant Reactor Core Neutronic Parameters Using Scale 6.1 Code

Dhirar Faisal Fajri<sup>a</sup>, Alexander Agung<sup>a,1</sup>, Andang Widi Harto<sup>a</sup>

<sup>a</sup>*Nuclear Energy Technology Laboratory, Department of Nuclear Engineering and Engineering Physics, Faculty of Engineering, Universitas Gadjah Mada, Jl. Grafika 2, Yogyakarta 55281, Indonesia  
E-mail: <sup>1</sup>a\_agung@ugm.ac.id*

**Abstract**— KLT-40S nuclear reactor is a small modular floating nuclear power plant made by Russia as a conventional light water reactor (LWR) problem solution nowadays, such as high overnight cost, long commissioning period, and lack of flexibility in supplying a small load of electricity and supplying electricity to isolated areas. With those characteristics, the KLT-40S is suitable to be applied to isolated areas with a small electrical load like archipelagic states such as Indonesia. Based on that reason, Indonesia needs to assess the KLT-40S floating nuclear power plant feasibility study through explorative research. One of those is assessing the reactor core neutronic parameter. In this research, the reactor core modelling is done by using the KENO VI-A and T-6DEPL module in SCALE 6.1 code package. Several variations of reactor operating parameters such as fuel composition and configuration, fuel temperature, moderator temperature, and moderator void fraction had been done in this research. The aim was to get several neutronic parameters to confirm the core feasibility from operational and inherent safety perspectives. Those neutronic parameters are fuel cycle length and reactivity feedback coefficient of fuel temperature, moderator temperature, and moderator void fraction. Based on this research result, the fuel configuration that produces 28 months of cycle length is the fuel base of dispersed UO<sub>2</sub> in the silumin matrix with 18,6 % <sup>235</sup>U enrichment. Both of the two fuel bases used in this research have inherent safety characteristics, which are shown by the negative value of the reactivity feedback coefficient of fuel temperature, moderator temperature, and moderator void fraction. Dispersed UO<sub>2</sub> in the silumin matrix fuel base has better inherent safety characteristics than the UO<sub>2</sub> ceramic metal fuel base.

**Keywords**— floating nuclear power plant; KLT-40S; silumin alloy; SCALE 6.1.

### I. INTRODUCTION

In general, the beginning of global and local Indonesian current energy problems is the increase in energy demand due to population growth and improved quality of life. Based on the United Nations projection data about the forecast of capita energy consumption, after 2010 energy consumption per capita will decrease due to an imbalance between growth in energy demand and energy production. Those data also concluded that global energy compliance is still dominated by fossil energy sources, which is the most significant contributor to global warming [1].

Nuclear (fission) energy is one of the best alternative options to replace fossil energy as the leading energy supplier that is environmentally friendly because it only produces 12 grams of CO<sub>2</sub> equivalent/kWh from commissioning until decommissioning [2]. Most nuclear power plants today are of Pressurized Water Reactor (PWR) type. Conventional PWRs have some disadvantages, such as high investment cost, long commissioning time, low flexibility in supplying small electrical loads, and low flexibility in supplying electrical loads in an isolated area.

For that reason, Russia then developed a small-capacity floating nuclear power plant called KLT-40S. KLT-40S is a PWR developed for floating nuclear power plants in which each reactor module produces 35 MWe power output. Nuclear island (including two modules reactor), turbine island, and all system of nuclear reactor support component placed inside the deck of a non-propulsion ship called Academic Lomonosov. Based on its history, KLT 40S is developed from the previous Russian floating reactor designs that are KLT-40 and KLT-40M. Both floating fission reactors were used to generate Tymyr Class icebreakers (KLT 40M, 171 MWatt) and to draw LASH (Lighter Aboard Ship) as well as an icebreaker (Sevmorput, KLT-40, 135 MWatt). Both reactors use uranium dioxide fuel with 30% to 40% <sup>235</sup>U Enrichment to produce the thermal power of 135 to 171 MW. FNPP with KLT-40S reactor can be manufactured in the shipyard and can be delivered to the customer in finished condition, tested, and ready to operate [3]. The summary of the design specifications of the KLT-40S reactor system is listed in Table 1 as follows:

TABLE I  
SUMMARY OF THE DESIGN SPECIFICATION OF KLT-40S REACTOR SYSTEM [4].

| Parameters   | Value                             |
|--|-----------------------------------|
| Thermal power output/module [MWt]                              | 150                               |
| Electric power output [MWe]                                    | 35                                |
| Core lifetime [year]   | 40                                |
| Availability [%]   | 85                                |
| Moderator material   | Light water                       |
| Thermodynamic cycle  | Indirect Rankine                  |
| Core active length [m]   | 1.2                               |
| Fuel material  | Uranium dioxide in silumin matrix |
| Lattice geometry   | Triangular                        |
| Fuel assembly pitch [mm]                                       | 100                               |
| Fuel element pitch [mm]  | 9.95                              |
| Cladding material  | Zircalloy-4                       |
| FE dimension across cladding, $\varnothing \times \delta$ [mm] | $6.8 \times 0.5$                  |
| Average $^{235}\text{U}$ enrichment [%]                        | 14.1                              |
| Burnable poison material                                       | $\text{Gd}_2\text{O}_3$           |
| Amount of gadolinium inside core [kg]                          | 46.3                              |
| Fuel cycle length [month]                                      | 28                                |
| Average fuel discharge burnup [GWd/MTU]                        | 45.4                              |
| Primary coolant inlet temperature [ $^{\circ}\text{C}$ ]       | 280                               |
| Primary coolant outlet temperature [ $^{\circ}\text{C}$ ]      | 316                               |
| Core operation pressure [MPa]                                  | 12.7                              |
| Inner RPV diameter [mm]  | 1920                              |
| RPV wall thickness [mm]  | 128                               |
| RPV total height [mm]  | 3892                              |
| RPV material   | Steel 15Cr2NiMo VA-A              |

The following is the fuel cycle used at the operation on KLT-40S. The first, Academic Lomonosov ship, in which the KLT-40S core filled with fresh fuel supply for 12 years' operations before being delivered to the customer. Upon arriving at the site, the FNPP KLT-40S will operate in each fuel cycle (once refueling) for 28 months, with an average fuel discharge burn-up of 45,4 GWd / MTU. After operating up to 28 months of all fuel assembly in the reactor will be replaced with a new fuel assembly without reshuffle. The cycle will be repeated until each reactor operates for 12 years, and the FNPP will be returned to the place of fabrication. The spent fuel from the previous 12-year operation will be discharged, and the FNPP will be loaded with new fuel for the next 12-year operation. Maintenance on the nuclear and turbine islands will also be performed thoroughly. With such a fuel cycle mechanism, FNPP KLT-40S does not require land transport infrastructure to supply fuel in isolated areas or remote areas [5].

Indonesia is an archipelagic and maritime state and is currently having situations such as the urgency of the 35,000 MWe government project, uneven electrification (centered on Java) and uneven infrastructure development. Considering those situations, Russia offers FNPP KLT-40S to Indonesia as a solution to produce electricity on the isolated and remote area in Indonesia. To assess this offer,

Indonesia needs to review the feasibility study of KLT-40S FNPP. Therefore, explorative research is needed to study KLT-40S characteristics; one of them is to study the neutronics of the reactor core.

The study related to the use of the KLT-40S system as a power plant and thermal energy supplier for seawater desalination has been done [6]. This study contained a feasibility test and an initial design of KLT-40S as a floating power plant for power generation and thermal energy for seawater desalination. It concluded that based on the technical and economic characteristics of KLT-40S when associated with existing desalination technology, the plant is declared feasible or can be implemented. Based on a preliminary design that has been made, seawater desalination with KLT-40S claimed to be able to produce clean water with a production capacity of  $20 \times 10^3$  to  $100 \times 10^3$  m<sup>3</sup>/day.

Another study of the hydrodynamic aspects at the fuel assembly-level has also been carried out by manufacturing a prototype of KLT-40S fuel device with the same geometry scale [7]. An experimental system was made by adding instrumentation and control aspects to the experimental model. The objective of the study was to obtain the hydrodynamic characteristics of the KLT-40S primary coolant at the local level (which is fuel assembly). Such hydrodynamic characteristic was obtained by measuring the local velocity on the fuel assembly water channel using the five-pressure probe on the fuel assembly model. The flow form and cooling turbulence properties were then obtained by using a tracer on the cooler.

Another study on the simulation of accident scenarios in terms of thermal-hydraulic aspects has been performed by modelling and normalizing the KLT-40S reactor system using SOCRATES thermal-hydraulic code [8]. Simulations using two main scenarios of accident phenomenon have been done: the first is the occurrence of the outbreak of the pipe on the ECCS (Emergency Core Cooling System), and then the second is the failure occurrence of the operation of the primary cooling loop. Safety analysis was done accordingly for those two accident scenarios.

Fuel with the uranium dioxide + aluminum alloy composition was developed for fuel elements to be used in floating power-generating units and small nuclear power plants. Designs, fabrication technologies, and methods of monitoring cermet fuel elements of different standard sizes with an aluminum matrix and cladding comprised of zirconium alloys were developed at the Bochvar All-Russia Research Institute for Inorganic Materials. A complex of pre-reactor and reactor tests and post-reactor studies of fuel elements was conducted [9]; it was shown that cermet fuel elements are promising. The particulars of the behavior under irradiation of fuel elements with the uranium dioxide + aluminum alloy fuel composition were determined.

Results of computer modelling of coolant flow in the fuel assembly of the reactor of a floating nuclear power plant using the LOGOS CFD programs have been given [10]. The possibility of using the obtained results to improve models built into the engineering programs of thermal-hydraulic calculation of nuclear-reactor cores has been considered.

Research on experimental investigations of local hydrodynamics of coolant flow in a fuel rod assembly (FA) of KLT-40S reactor behind a plate spacer grid has been done,

and the result has been presented [11]. The investigations were carried out on an aerodynamic rig using the gas-phase diffusive tracer test. An analysis of the spatial distribution of absolute low-velocity projections and distribution of tracer concentration allowed specifying a coolant flow pattern behind the plate spacer grid of the FA. Based on obtained experimental data, the recommendations were provided to specify procedures for determining the coolant flow rates for the programs of cell-wise calculation of a core zone of the KLT-40S reactor. Investigation results were accepted for the practical use in JSC "OKBM Afrikantov" to assess heat engineering reliability of the KLT-40S reactor core and were included in a database for verification of CFD programs (CFD-codes).

Research on neutronic aspects at the fuel assembly-level has been done to study the multiplication factor and the breeding ratios of the KLT-40S core under operating conditions [12]. The study was conducted by varying the composition of fissile and fertile nuclides in KLT-40S fuel. Variations were performed with four options of fertile-fissile nuclide pairs: (i) ( $^{238}\text{U} + ^{235}\text{U}$ ) pair which is the basis design of KLT-40S made by OKBM Afrikantov, (ii) ( $^{238}\text{U} + ^{239}\text{Pu}$ ) pair, (iii) ( $^{232}\text{Th} + ^{235}\text{U}$ ) pair and (iv) ( $^{232}\text{Th} + ^{233}\text{U}$ ) pair. The four options of the nuclide composition were modelled in oxide-based or ceramic-fueled fuels, which were dispersed into an inert silumin alloy matrix with the fissile nuclide content of the four options having a maximum weight fraction of 18.6%. The calculation of multiplication factor and the breeding ratios was done by computational iterative equations, resulting in the most optimal fuel option to be the combination between ( $^{232}\text{Th} + ^{233}\text{U}$ ).

Based on previous research, research on the neutronic aspects of the KLT-40S reactor core is still rare. Research carried out by Baybakov *et al.* [12] is a neutronic aspect of the KLT-40S reactor but is only limited to the level of fuel assembly with uniform fissile content enrichment. Therefore, it is necessary to investigate further neutronic aspects of the KLT-40S reactor nuclear reactor, considering the full core configuration arrangement to obtain more accurate neutronic parameters.

In our research, the KLT-40S core with 121 fuel assemblies, each of which contained 69 to 75 fuel elements and burnable poison rods, was modelled by using SCALE 6.1 neutronic code with KENO VIA module for reactivity and safety analysis and T-6DEPL module for burn-up and depletion analysis. The fuel used in this research is  $\text{UO}_2$  cermet and dispersed  $\text{UO}_2$  in silumin alloy and the burnable poison rod modelled with a mixture of  $\text{UO}_2$ ,  $\text{Gd}_2\text{O}_3$ , and silumin alloy.

This study has the following objectives:

1. To obtain the cycle length of each fuel and core configuration that is modelled in this research,
2. To obtain the appropriate  $^{235}\text{U}$  fuel enrichment level to produce cycle length approaching (fuel cycle length claim) 28 months,
3. To obtain the inherent safety neutronic performance characteristic of the KLT-40S reactor.

## II. MATERIAL AND METHOD

The thermal neutron multiplication factor (denoted as  $k$ ) is defined as the ratio of the number of thermal neutrons

absorbed by the fuel in a neutron cycle to the number of thermal neutrons absorbed by the fuel in the previous cycle. The value of the neutron thermal multiplication factor can be written as:

$$k = \eta \epsilon p f P_f P_t \quad (1)$$

The value of ( $k$ ) is the criticality of the reactor. If  $k=1$ , then the reactor is in critical condition with a constant fission reaction rate over time. If  $k>1$ , then the reactor is in supercritical condition with the rate of fission reaction increases with time. If  $k<1$ , then the reactor is subcritical with fission reaction rate decreases over time.  $\eta$  is called the thermal fission factor, and it states the average number of fast neutrons produced per absorption of a thermal neutron by fuel.  $\epsilon$  is defined as a fast fission factor, which is the ratio of all fission reactions both induced by both thermal neutrons and fast neutrons to fission reactions induced by only thermal neutrons.  $p$  is the fast neutrons resonance escape probability. The thermal utilization factor ( $f$ ) is defined as the ratio of the thermal neutron absorbed by the fuel to the overall thermal neutron absorbed by moderators, coolants, structures and neutron-absorbing materials for the control of the reactor.  $P_f$  and  $P_t$ , respectively, are fast and thermal neutron non-leakage probability. Taking into account the  $^{235}\text{U}$  depletion, burnable poison depletion and the formation of  $^{239}\text{Pu}$  when the reactor is operated, Eq (1) can be written as [13]

$$k(t) = \frac{(v\sigma_f^{25}N^{25}(t) + v\sigma_f^{49}N^{49}(t))\epsilon p P_f P_t}{\sigma_a^{25}N^{25}(t) + \sigma_a^{49}N^{49}(t) + \Sigma_a^{28}(t) + \zeta \left(\frac{V^M}{V^F}\right) \Sigma_a^M + N^{BP}(t)\sigma_c^{BP}} \quad (2)$$

where the superscripts 25, 49, and 28 respectively are indexes for  $^{235}\text{U}$ ,  $^{239}\text{Pu}$  and  $^{238}\text{U}$ ,  $\zeta$  is a thermal disadvantage factor which expresses the ratio of average neutron flux in a moderator to average neutron flux in fuel. In general,  $\zeta$  is larger than one.

Changes in fuel and moderator temperatures can affect the multiplication factor value of the fission reactor system. The phenomenon of changes in the reactivity or multiplication factor due to changes in operating parameters is called reactivity feedback. The effect of temperature change on the reactivity of a nuclear reactor is expressed in the temperature reactivity feedback. The temperature reactivity coefficient is defined as the fraction of the criticality change to the temperature change. The empirical approach to fuel temperature reactivity coefficient (FTC) with uranium base is expressed in the following equation [13]:

$$\alpha_{Tf} = \ln \left( \frac{1}{p(300K)} \right) \frac{\beta'''}{2\sqrt{T_F(K)}} \quad (3)$$

where  $\beta'''$  for uranium fuel base is as follows:

$$\beta''' = 61 \times 10^{-4} + 47 \times 10^{-4} \left( \frac{S_F}{M_F} \right) \quad (4)$$

The following equation expresses the simple theoretical approach to moderator temperature reactivity coefficient (MTC):

$$\alpha_{Tm} = -\ln p \left( \frac{1}{N_M} \frac{\partial N_M}{\partial T_M} \right) \quad (5)$$

$$p = e^{-\frac{N_f V_f \Gamma}{\xi^{2s,m} V_m}} \quad (6)$$

The following equation expresses the simple theoretical approach to moderator void reactivity coefficient (VRC):

$$\alpha_\vartheta = \ln p \left( \frac{1}{N_M} \frac{\partial N_M}{\partial \vartheta} \right) \quad (7)$$

The initial phase of this study was modelling the KLT-40S fuel assembly by the IAEA ARIS document reference [4]. Fuel assembly and core dimensions were made fixed because there was no analysis of geometry variations in this research. The design of the fuel assembly was made by using the GEEWIZ KENO-VI A module, as shown in Figure 1 and The geometry and material details of fuel assembly are listed in Table 2.

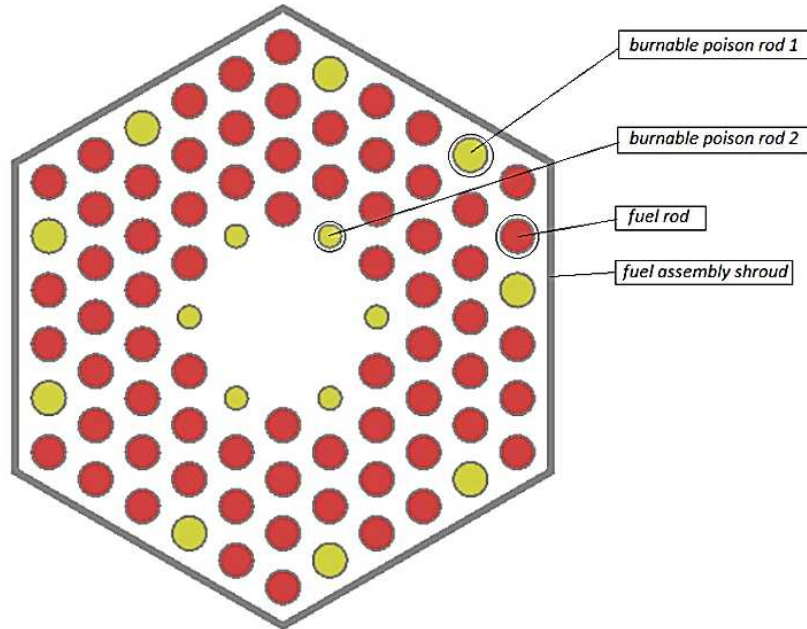


Fig. 1 Fuel assembly model top view

TABLE II  
FUEL ASSEMBLY MODEL GEOMETRY SPECIFICATION

| Parameter (material)  | Dimension [cm] |
|---|----------------|
| Fuel rod outer diameter   | 0.34           |
| Cladding thickness on fuel rods and burnable poison rods (Zircaloy-4) | 0.5            |
| Fuel element lattice pitch  | 0.995          |
| Burnable poison rod 1 outer radius                                    | 0.34           |
| Burnable poison rod 2 outer radius                                    | 0.238          |
| Fuel assembly active height   | 120            |
| The outer side length of fuel assembly hexagon                        | $10/\sqrt{3}$  |
| Shroud thickness (Zircaloy-4)   | 0.15           |

This research used two different fuel bases, i.e.,  $UO_2$  cermet and dispersed  $UO_2$  in silumin matrix. From the calculation results with several assumption approaches, material compositions for each base were obtained and listed in Table 3.

TABLE III  
MATERIAL DATA OF FUEL ROD AND BURNABLE POISON ROD

| Composor material | Density [g/cm <sup>3</sup> ] | Cermet-based volume fraction |                     | Dispersed $UO_2$ -based volume fraction |                     |
|-------------------|------------------------------|------------------------------|---------------------|---|---------------------|
|                   |                              | Fuel rod                     | Burnable poison rod | Fuel rod                                | Burnable poison rod |
| $UO_2$            | 10.96                        | 1                            | 0.852               | 0.436                                   | 0.371               |
| Silumin alloy     | 7.07                         | 0                            | 0                   | 0.564                                   | 0.481               |
| $Gd_2O_3$         | 3                            | 0                            | 0.148               | 0                                       | 0.148               |

The silumin alloy composition being used in the model are listed in Table 4.

TABLE IV  
SILUMIN ALLOY COMPOSITION

| Element | Mass fraction [%] |
|---------|-------------------|
| Si      | 10.0              |
| Fe      | 0.15              |
| Cu      | 0.03              |
| Mn      | 0.1               |
| Mg      | 0.4               |
| Zn      | 0.07              |
| Ti      | 0.15              |
| Al      | 89.1              |

The design of the fuel assembly, as illustrated in Figure 1, was then arranged in a full core configuration (triangular lattice) with a pitch distance of 10 cm, as shown in Figure 2, with a simplification that the core contains only up to two types of fuel assembly enrichment. Figure 2 is an example of a core arrangement with two types of fuel assembly being modelled.

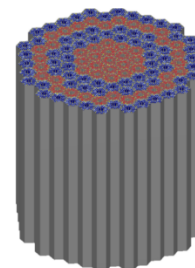


Fig. 2 Full core configuration model for two types of the fuel assembly

The core was placed into the reactor vessel. Figure 3 shows the dimensions of the vessel and the placement of the core.

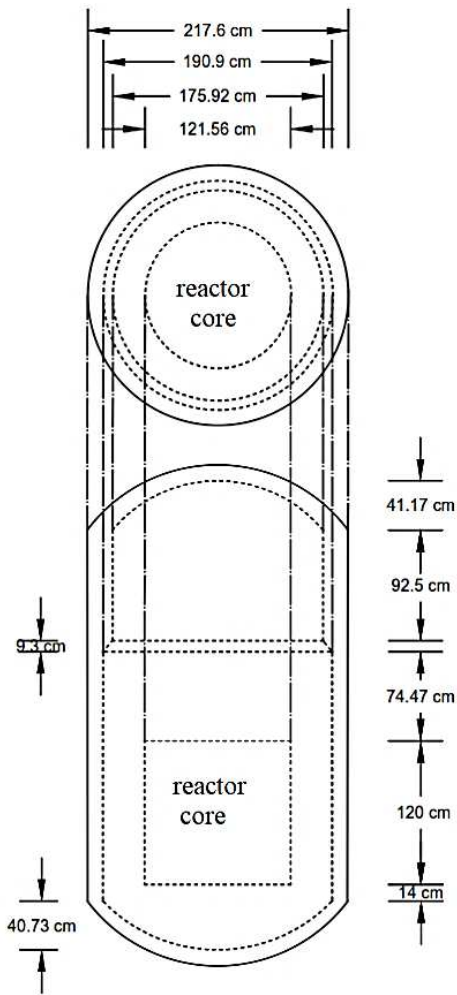


Fig. 3 The projection image of the top and front view of the reactor vessel model with the position of the core inside

The reactor vessel was made from 15Cr2NiMo VA-A steel alloy type with the detail of the composition, as shown in Table 5.

TABLE V  
15Cr2NiMo VA-A ALLOY COMPOSITION

| Element | Mass fraction (%) |
|---------|-------------------|
| C       | 0.15              |
| Si      | 0.26              |
| Mn      | 0.42              |
| S       | 0.012             |
| P       | 0.008             |
| Cr      | 2.11              |
| Ni      | 1.22              |
| Mo      | 0.57              |
| V       | 0.1               |
| Cu      | 0.07              |
| Fe      | 95.07             |

Figure 4 shows the configuration of the whole core vessel modelled.

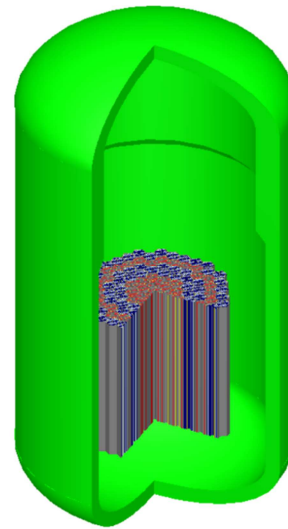


Fig. 4 The 3D image with a quarter slice of reactor core and vessel.

Within this research, there were several variations of independent variables, namely variations of fuel configuration, fuel temperature, moderator void fraction and moderator temperature with detail variation of each parameter shown in Table 6, 7, 8 and 9.

TABLE VI  
VARIATION OF FUEL CONFIGURATION

| No. Variation | <sup>235</sup> U Enrichment (%)     | Fuel base   |
|---------------|-------------------------------------|---|
| 1             | 15.7                                | UO <sub>2</sub> ceramic                                 |
| 2             | 18.6                                |   |
| 3             | 19.95                               |   |
| 4             | 15.7 & 18.6<br>(2 FA types in core) | UO <sub>2</sub> dispersed in inert matrix silumin alloy |
| 5             | 15.7                                |   |
| 6             | 18.6                                |   |
| 7             | 19.95                               |   |
| 8             | 15.7 & 18.6 (2 FA types in core)    |   |

TABLE VII  
VARIATION OF FUEL TEMPERATURE

| No. variation | <sup>235</sup> U enrichment (18,6%) |   |
|---------------|-------------------------------------|---|
|               | Fuel temperature (Kelvin)           | Fuel base   |
| 1             | 300                                 | UO <sub>2</sub> cermet                                  |
| 2             | 350                                 |   |
| 3             | 400                                 |   |
| 4             | 450                                 |   |
| 5             | 500                                 |   |
| 6             | 550                                 |   |
| 7             | 600                                 |   |
| 8             | 650                                 |   |
| 9             | 700                                 |   |
| 10            | 750                                 |   |
| 11            | 800                                 |   |
| 12            | 300                                 | UO <sub>2</sub> dispersed in inert matrix silumin alloy |
| 13            | 350                                 |   |
| 14            | 400                                 |   |
| 15            | 450                                 |   |
| 16            | 500                                 |   |
| 17            | 550                                 |   |
| 18            | 600                                 |   |
| 19            | 650                                 |   |
| 20            | 700                                 |   |
| 21            | 750                                 |   |
| 22            | 800                                 |   |

TABLE VIII  
VARIATION OF MODERATOR VOID

| No. variation | Void fraction (%) | Coolant density (gram/cc) | Fuel base   |
|---------------|-------------------|---------------------------|---|
| 1             | 0                 | 0.64733                   | UO <sub>2</sub> cermet                                  |
| 2             | 5                 | 0.61870                   |   |
| 3             | 10                | 0.59008                   |   |
| 4             | 15                | 0.56145                   |   |
| 5             | 20                | 0.53282                   |   |
| 6             | 25                | 0.50420                   |   |
| 7             | 0                 | 0.64733                   | UO <sub>2</sub> dispersed in inert matrix silumin alloy |
| 8             | 5                 | 0.61870                   |   |
| 9             | 10                | 0.59008                   |   |
| 10            | 15                | 0.56145                   |   |
| 11            | 20                | 0.53282                   |   |
| 12            | 25                | 0.50420                   |   |

TABLE IX  
VARIATION OF MODERATOR TEMPERATURE

| No. variation | Coolant temperature (Kelvin) | Coolant density (gram/cc) | Fuel base   |
|---------------|------------------------------|---------------------------|---|
| 1             | 300                          | 1.00213                   | UO <sub>2</sub> cermet                                  |
| 2             | 350                          | 0.97926                   |   |
| 3             | 400                          | 0.94374                   |   |
| 4             | 450                          | 0.89785                   |   |
| 5             | 500                          | 0.84039                   |   |
| 6             | 550                          | 0.76576                   |   |
| 7             | 600                          | 0.65083                   |   |
| 8             | 300                          | 1.00213                   | UO <sub>2</sub> dispersed in inert matrix silumin alloy |
| 9             | 350                          | 0.97926                   |   |
| 10            | 400                          | 0.94374                   |   |
| 11            | 450                          | 0.89785                   |   |
| 12            | 500                          | 0.84039                   |   |
| 13            | 550                          | 0.76576                   |   |
| 14            | 600                          | 0.65083                   |   |

Neutronic calculations were performed using a stochastic computational method (Monte Carlo) in KENO-VIA and T-6DEPL modules of SCALE 6.1 package code. After the input code of SCALE 6.1 was set, the running process was then performed through GEEWIZ parallel. Running process was done to get the parameters needed in this research, i.e. burn-up value, cycle length and multiplication factor. After all parameter were obtained, then the output data is processed for further analysis.

### III. RESULTS AND DISCUSSION

#### A. Multiplication Factor and Fuel Cycle Length

The first parameter to be analyzed is the core excess multiplication factor as a function of fuel depletion time or burn-up time. From the excess multiplication factor plot to the time function, the cycle length of the defined fuel configuration can be determined. The  $k_{eff}$  simulation result as a function of time is presented in two separate plot groups based on the fuel base used in this research. Figures 5 and 6 show the plot of each fuel configuration  $k_{eff}$  as a function of burn-up time. The multiplication factor value is directly proportional to the rate of fission reaction occurring in the

core and inversely proportional to the overall neutron absorption rate in a fission reactor system.

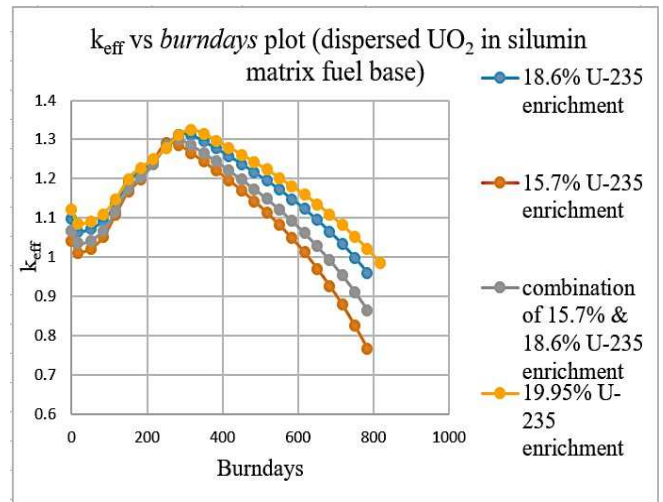


Fig. 5  $k_{eff}$  vs burndays plot for UO<sub>2</sub> in silumin matrix fuel base.

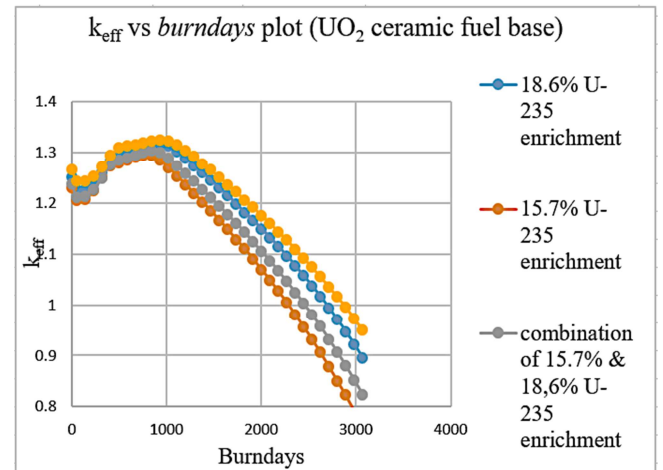


Fig. 6  $k_{eff}$  vs burndays plot for UO<sub>2</sub> ceramic fuel base.

From Figures 5 and 6, all fuel configurations have an excess criticality value of more than one at the beginning-of-cycle (or in supercritical condition). It means all fuel configuration variations have the ability to maintain the continuity of the fission chain reaction on the system without the addition of an external neutron source. It can also be observed from Figures 5 and 6 that the higher <sup>235</sup>U enrichment on the same fuel base, then the  $k_{eff}$  value will also increase. That phenomenon is in accordance with the 6-factor formula for multiplication factor: the increase of <sup>235</sup>U enrichment resulted in the increase of  $\eta$ . Thermal neutron reproduction factor ( $\eta$ ) is directly proportional to the value of  $\Sigma_{f,T,F}$  which is the fission macroscopic cross-section of the fuel. The higher <sup>235</sup>U enrichment level result in an increase of fissile density in the fuel and density of fertile <sup>238</sup>U will decrease so the value of  $\Sigma_{f,T,F}$  will increase,  $\Sigma_{a,T,F}$  will decrease,  $\eta$  will increase, and the integral resonance  $p$  will decrease so the multiplication factor will increase.

From Figures 5 and 6 it can be observed that the value of  $k_{eff}$  UO<sub>2</sub> ceramic fuel base is relatively much more substantial than dispersed UO<sub>2</sub> fuel base on the same <sup>235</sup>U enrichment level. This result can be explained by several

reasons, including the difference in fuel structure due to the existence of silumin alloy and the difference in the volume fraction of  $\text{UO}_2$  contained in fuel and burnable poison rods. On ceramic fuel base  $\text{UO}_2$  is fully loaded in fuel rod while on dispersed  $\text{UO}_2$  fuel base,  $\text{UO}_2$  is partially loaded in fuel rod with 0.4356 volume fraction that means it has a brief value of  $\Sigma_{f,T,F}$  0.4356 times less than  $\text{UO}_2$  ceramic fuel base, so that the value of  $\eta$  and  $k_{\text{eff}}$  is less than pure  $\text{UO}_2$  ceramics fuel base.

The presence of silumin in dispersed  $\text{UO}_2$  fuel base also decreases the thermal utility factor  $f$ . However, the effect of the addition of system absorption macroscopic cross-section due to the addition of structural material such as silumin is minimal and even negligible. It is because aluminum and silicon as the main constituent element of silumin alloy have a low neutron absorption microscopic cross-section. Aluminum has a neutron absorption microscopic cross-section of 0.232 barns, while silicon has only 0.171 barns.

Four profiles of each plot have a relatively similar trend. Starting from the zeroeth time step to the first time step, the  $k_{\text{eff}}$  value will decrease. Between the zeroeth and first time step, fission products Xenon-135 and Samarium-149 is forming and reaches their saturated levels. Those two fission products are regarded as neutron poison because of their very large neutron absorption cross-section. After the  $k_{\text{eff}}$  value decrease between the zeroeth time step and the first timestep, then the  $k_{\text{eff}}$  value will increase towards the peak value. Such an increase in the  $k_{\text{eff}}$  is caused by the depletion of burnable poison and the formation of  $^{239}\text{Pu}$ . Such reactivity increase outweighs the reactivity decrease due to the depletion of the  $^{235}\text{U}$  fissile nuclides. Within the next phase after the peak  $k_{\text{eff}}$  has been achieved, there will be a continuous decrease in the  $k_{\text{eff}}$  values. In this phase the burnable poison concentration is very low so the concentration disintegration rate of gadolinium also very low, the formation of the fissile isotope plutonium continues. However, the rate of its formation also decreases so that the influence of  $^{235}\text{U}$  depletion dominates the change or decrease in  $k_{\text{eff}}$  value in this phase.

The decrease in  $k_{\text{eff}}$  values will occur continuously until the fuel is declared cannot be utilized again to support the occurrence of fission chain reaction. The fuel is declared exhausted (end-of-cycle) when the value of core excess multiplication factor less than or equal 1. The time from the beginning-of-cycle to the end-of-cycle is expressed as the fuel cycle length. Within this research, the fuel cycle length can be determined by finding the intersection between each time-dependent  $k_{\text{eff}}$  plot curve and a horizontal line representing  $k_{\text{eff}}$  equals 1. The result shows the cycle length of each fuel configuration as shown in Table 10.

The KLT-40S fuel cycle length was claimed to be able to reach 28 months or within the range of 2 to 3 years [3]. Based on Table 8, dispersed  $\text{UO}_2$  fuel base with 18.6% and 19.95%  $^{235}\text{U}$  enrichment have a cycle length range between 2 to 3 years. Meanwhile, the cycle length of  $\text{UO}_2$  ceramic fuel is too long (i.e., 6 to 7 years). Based on IAEA ARIS data of KLT-40S fuel [4], KLT-40S fuel base on FOAK (First of a Kind) status is the same as conventional PWR fuel that is uranium fuel based on ceramic oxide  $\text{UO}_2$ . A possible discrepancy in the  $\text{UO}_2$  ceramic fuel base model against the FOAK status claim is possibly caused by the use of

conventional PWRs  $^{235}\text{U}$  enrichment level (3% to 7%) on the status of FOAK. The  $^{235}\text{U}$  enrichment of 19.95% is the maximum enrichment limit before violating the existing safeguard rules of 20%. The practical approach of 19.95% average  $^{235}\text{U}$  enrichment cannot be implemented. Assume that there are 5 up to 8 types of FA having different  $^{235}\text{U}$  enrichments, and they constitute an average core enrichment level of 19.95%. It is undoubtedly that some FAs in the core contain  $^{235}\text{U}$  enrichment level above 20% and hence the existing safeguard limits will be violated. Therefore, dispersed  $\text{UO}_2$  in silumin matrix fuel base with 18.6% average  $^{235}\text{U}$  enrichment is capable of producing a cycle length of 28 months, although the simulation results in 24.6 months' cycle length only. This inability to achieve the 28-month cycle length is justifiable as the reactor was modeled by using only one type of  $^{235}\text{U}$  enrichment level in the fuel assembly. Moreover, the simulated model also ignores the existence of a core barrel due to limited data obtained from open literature. It is possible with the existence of a core barrel that the non-leakage probability of thermal neutron and fast neutron will increase ( $P_f$  and  $P_t$ ) because the core barrel can act as a reflector. The  $k_{\text{eff}}$  excess value consequently will increase at the beginning of the cycle and the cycle length may also increase.

TABLE X  
CYCLE LENGTH OF EACH FUEL CONFIGURATION

| Fuel base                                 | $^{235}\text{U}$ enrichment | Cycle length |        |       |
|---|-----------------------------|--------------|--------|-------|
|   |                             | Days         | Months | Years |
| Ceramic $\text{UO}_2$                     | 15.7%                       | 2285.63      | 75.14  | 6.26  |
|   | 15.7% and 18.6%             | 2455.38      | 80.72  | 6.73  |
|   | 18.6%                       | 2687.30      | 88.35  | 7.36  |
|   | 19.95%                      | 2871.77      | 94.41  | 7.87  |
| Dispersed $\text{UO}_2$ in silumin matrix | 15.7%                       | 626.33       | 20.59  | 1.72  |
|   | 15.7% and 18.6%             | 675.56       | 22.21  | 1.85  |
|   | 18.6%                       | 748.31       | 24.60  | 2.05  |
|   | 19.95%                      | 803.24       | 26.41  | 2.20  |

### B. Inherent Safety Aspect (Reactivity Feedback Coefficient)

1) *Variation of Fuel Temperature:* Figures 7 and 8 show the results of variations in fuel temperature to the reactivity for different fuel base.

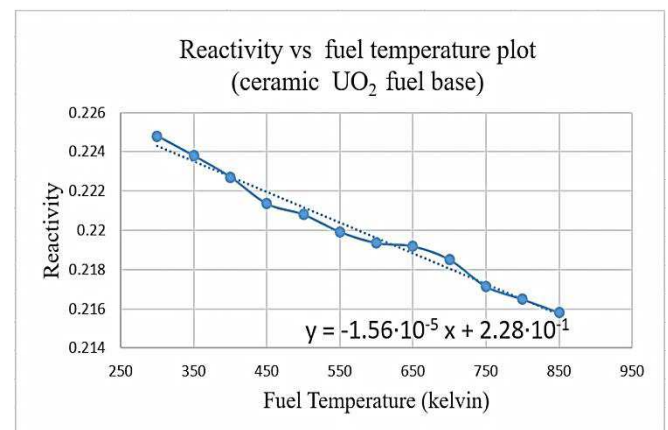


Fig. 7 Reactivity vs fuel temperature plot for ceramic  $\text{UO}_2$  fuel base.

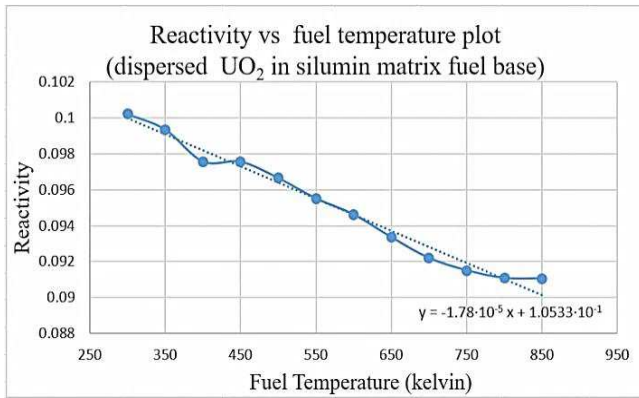


Fig. 8 Reactivity vs fuel temperature plot for dispersed  $\text{UO}_2$  in silumin matrix fuel base

The fuel temperature reactivity feedback can be obtained from a linear regression equation of each plot in Figure 7 and 8. The gradient from the linear regression represents the feedback coefficient. Both fuel configurations have negative reactivity coefficient values, indicating an inherent safety aspect of the configuration when the fuel temperature condition rises. Each increase of 1 Kelvin at the fuel temperature will give negative reactivity feedback of -1.56 pcm reactivity for  $\text{UO}_2$  ceramic fuel base and -1.78 pcm for dispersed  $\text{UO}_2$  in silumin matrix fuel base. Such an increase implies a decrease in the reactivity of the core as fuel temperature increases. The continuous decline in the value of reactivity due to this increase in fuel temperature can be understood through the theory of Doppler effects. An increase in fuel temperature will result in the widening of the resonance spectrum of the neutron absorption microscopic cross-section of the fuel in the epithermal energy range. Consequently, the resonance escape probability decreases, leading to a decrease in reactivity.

The FTC for the  $\text{UO}_2$  ceramic fuel bases and the dispersed  $\text{UO}_2$  in the silumin matrix, respectively of -1.56 pcm/K and -1.78 pcm/K are less than the  $\alpha_{Tf}$  range of conventional PWR, i.e. 2 pcm/K to -5 pcm/K. These smaller values are understandable as both fuel configurations have higher  $^{235}\text{U}$  enrichment levels than conventional PWRs (3% to 7%). The more fissile density contained in the fuel will result in a lower resonance absorption cross-section spectrum, so that the resonance integral value will decrease. The lower resonance integral value will also result in the decrease of  $\frac{\partial I}{\partial T_f}$ , and consequently those will result in a lower absolute value of  $\alpha_{Tf}$ .

Both types of fuel configurations produce different  $\alpha_{Tf}$  values. The absolute value of  $\alpha_{Tf}$   $\text{UO}_2$  based dispersion fuel in the silumin matrix is higher than that of the  $\text{UO}_2$  ceramic fuel base. This higher value can be understood by reviewing the empirical equations approach to determine  $\alpha_{Tf}$  (i.e., Eq. 3 and 4). Dispersed  $\text{UO}_2$  in the silumin matrix fuel base has lighter fuel elements total mass than the  $\text{UO}_2$  ceramic fuel base, with the same fuel element surface area, thus having a larger value of  $\frac{S_F}{M_F}$  and  $\beta'''$  causes the absolute value of  $\alpha_{Tf}$  becomes larger.

1) Variation of moderator void: Figures 9 and 10 show the results of variations in moderator void fraction to the reactivity for different fuel base.

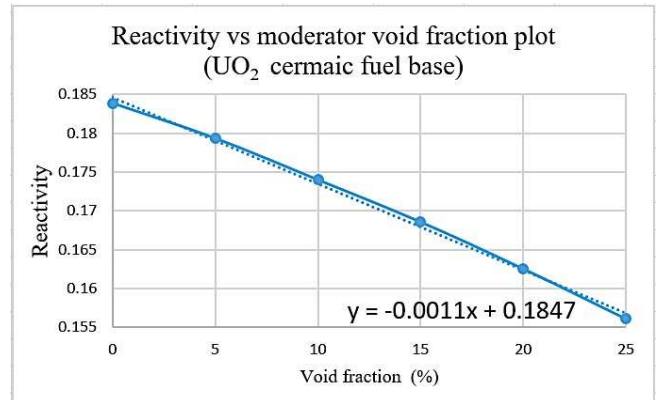


Fig. 9 Reactivity vs moderator void fraction plot for the  $\text{UO}_2$  ceramic fuel base.

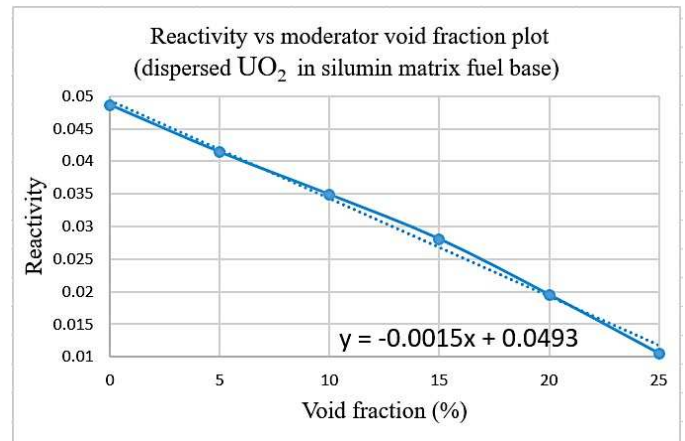


Fig. 10 Reactivity vs moderator void fraction plot for the dispersed  $\text{UO}_2$  in silumin matrix fuel base.

The values of the VRC of both fuel configurations above are negative. This fact is particularly important regarding the inherent safety aspects of boiling or steam bubble formation in the reactor core primary coolant. The negative value of VRC indicates that should an increase in the steam bubble population occur, the reactivity of the core will decrease. Consequently, this reactivity decrease will lead the reactor power and the fuel temperature and moderator to decrease as well and prevent a further boiling process. Keeping the heat from the fuel through the coolant is essential. The declining value of core reactivity due to an increased void fraction might be caused by the under-moderated condition of the modeled fuel configuration. As the void fraction rises it will cause the density of the moderator to decrease. This decrease in density results in a decrease in the thermal neutron population due to the less moderation process. The resonance escape probability decreases as well, and consequently the  $k_{eff}$  value will decrease.

Based on Figures 9 and 10, the value of VRC for  $\text{UO}_2$  ceramic fuel base is -110 pcm/% void and for dispersed  $\text{UO}_2$  in silumin matrix fuel base is -150 pcm/% void. Differences in the VRC values where dispersion-based fuel configuration has larger absolute value due to the difference in the number



of nuclide  $^{235}\text{U}$  populations used by both types of fuel.  $\text{UO}_2$  ceramic fuel base has a larger quantity of  $^{235}\text{U}$  than a dispersion-based fuel. So the value of the moderator-to-fuel ratio on the dispersion fuel is larger than the purely  $\text{UO}_2$  ceramic fuel base. The decrease of multiplication factor caused by the increase of coolant void fraction is dominated by neutron spectrum hardening event due to the decrease of moderator density. Therefore, the system with a larger  $N_m/N_u$  ratio will decrease significantly if there is a decrease in moderator density. Both values of VRC obtained have a slightly larger absolute value than conventional PWRs worth about -100 pcm/% void. Such a difference is caused by distinct operational pressure between conventional PWRs and KLT-40s. The conventional PWR works at an operating pressure of about 16 MPa, while KLT-40S has 12.7 MPa operating pressure. The difference between water and steam density on 16 MPa is smaller than the difference between water and steam density at 12.7 MPa. Thus the change in moderator coolant density due to changes in a void fraction at a pressure of 12.7 MPa is well larger than at a pressure of 16 MPa, resulting in a larger reactivity changes at the same increase of void fraction.

2) *Variation of moderator temperature*: Figures 11 and 12 show the results of variations in moderator temperature to the reactivity for different fuel base.

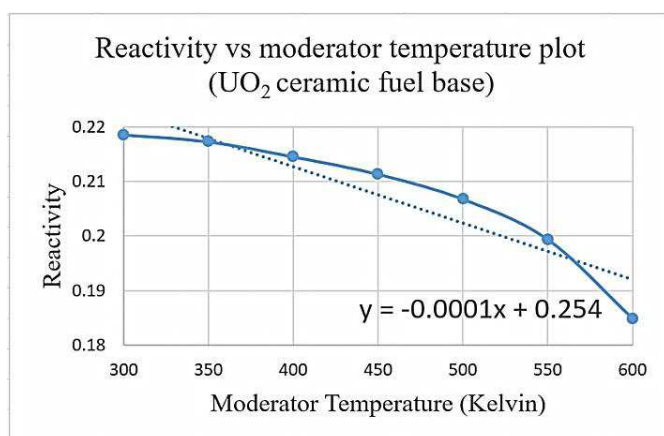


Fig. 11 Reactivity vs moderator temperature plot for the  $\text{UO}_2$  ceramic fuel base.

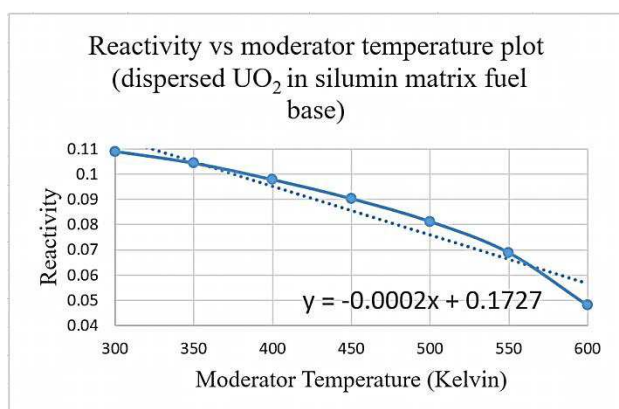


Fig. 12 Reactivity vs moderator temperature plot for the dispersed  $\text{UO}_2$  in silumin matrix fuel base.

From Figures 11 and 12, the values of both the MTCs for each fuel base are negative, which means if the moderator

temperature rises, the value of the reactivity of the core will decrease. This fact is particularly important concerning the inherent safety aspects and control of the reactor. The declining value of reactivity due to rising temperatures of moderators is identical to the phenomenon in which the void population increase, as described in the previous section. Briefly, the same as the previous discussion that the reactor is designed under under-moderated conditions so that if there is a decrease in moderator density, the value of  $k_{eff}$  or reactivity will decrease. There is a difference between moderator void reactivity feedback and moderator temperature reactivity feedback. The VRC explains the phenomenon of reactivity change due to the boiling process. In contrast, the MTC explains the phenomenon of reactivity change due to temperature rise, which causes thermal expansion of moderators before boiling occurs. The moderator thermal expansion will reduce the resonance probability value that impacts the decline in the reactivity value. The MTC values of each fuel base are -10 pcm/K for  $\text{UO}_2$  ceramic and -20 pcm/K for dispersed  $\text{UO}_2$  in the silumin matrix fuel base. This difference is due to the dispersed  $\text{UO}_2$  fuel base has smaller fuel element density than the  $\text{UO}_2$  ceramic fuel base. It can be understood through Equations 5 and 6 that should the density of heavy metal nuclides in the fuel ( $^{238}\text{U}$  and  $^{235}\text{U}$ )  $N_f$  decrease, the resonance escape probability  $p$  will increase. The higher the value of  $p$ , the higher the absolute value of  $\alpha_{Tm}$  will be. Therefore the absolute value of  $\alpha_{Tm}$  on dispersed  $\text{UO}_2$  in the silumin matrix fuel base is greater than on the  $\text{UO}_2$  ceramic fuel base.

After all reactivity feedback coefficients were obtained for both fuel base, it can be seen that dispersed  $\text{UO}_2$  in the silumin matrix fuel base has a higher absolute value of  $\alpha_{Tf}$ ,  $\alpha_\theta$  and  $\alpha_{Tm}$  than the conventional  $\text{UO}_2$  ceramic fuel base. It shows that the fuel design used by KLT-40S with dispersed  $\text{UO}_2$  in the inert metal matrix fuel base has a better inherent safety aspect than the conventional PWR fuel base (ceramic  $\text{UO}_2$ ).

#### IV. CONCLUSION

The fuel cycle length for  $\text{UO}_2$  ceramic fuel base with 15.7%, 15.7% and 18.6%, 18.6%, and 19.95% enriched  $^{235}\text{U}$  respectively of 75.1441 months, 80.7249 months, 88.3495 months, and 94.4144 months, while for dispersed  $\text{UO}_2$  fuel base with  $^{235}\text{U}$  enrichment of 15.7%, 15.7% and 18.6%, 18.6%, and 19.95% respectively of 20.5917 months, 22.2103 months, 24.6019 months, and 26.4078 months. The fuel base and the average fuel enrichment to achieve a fuel assembly configuration design and a 28-month cycle length as claimed are the silumin-based (cermet) fuels with an average enrichment rate of 18.6%. KLT-40S reactor with  $\text{UO}_2$  ceramic and dispersed  $\text{UO}_2$  fuel base have inherent safety aspect because it has negative reactivity coefficient of fuel temperature, moderator temperature, and void. The results of the distribution of plutonium isotopes in all configurations have a reasonably good proliferative resistance because they belong to the reactor-grade plutonium category.

#### ACKNOWLEDGMENT

This research was supported by the Department of Nuclear Engineering and Engineering Physics Faculty of Engineering, Universitas Gadjah Mada, Yogyakarta through Dana Masyarakat UGM of Fiscal Year 2017.

#### REFERENCES

- [1] United Nations, *The 2015 Revision of World Population Prospects*, Department of Economic and Social Affairs, New York, 2015.
- [2] T. Bruckner, *Technology-specific Cost and Performance Parameters*, Cambridge University Press, Cambridge, 2014.
- [3] Standing, Mark Dowdal, and William J.F, *Floating Nuclear Power Plant and Associated Technologies in the Northern Areas*, Norwegian Radiation Protection Authority, Østerås, 2008.
- [4] International Atomic Energy Agency, *Status Report 73 - KLT-40S*, IAEA, Vienna, 2010.
- [5] OKBM Afrikantov, KLT-40S Reactor Plants for Small Nuclear Plants, Nizhny Novgorod: OKBM Afrikantov.
- [6] V. I. Kostin, Yu.K. Panov, V. I. Polunichev, and I. E. Shamamin, "Floating Power Generating Unit with a KLT-40S Reactor System for Desalinating Seawater", *Atomic Energy*, vol. 1, no. 102, pp. 31-35, 2007.
- [7] S.M. Dmitriev, A.V. Varentsov, A.A. Dobrov, D. V. Doronkov, A. N. Pronin, V. D. Sorokin, and A. E. Khrobostov, "Computational and Experimental Investigations of the Coolant Flow in the Cassette Fissile Core of a KLT-40S Reactor", *Journal of Engineering Physics and Thermophysics*, vol.90, no. 4, pp. 941-950, 2017.
- [8] S. M. Dmitriev, A. V. Varentsov, D. V. Doronkov, M.A. Leghchanov, and D. N. Solentsev, "Calculation Studies Severe Accident KLT-40s", *Materialy Konferentsii KMS*, chapter 1, article no. 16, Podolsk, 2012.
- [9] G. V. Kulikalov, A. V. Vatulin, S. A. Ershov, Yu. V. Konovalov, A. V. Morozov, V. I. Sorokin, V. V. Fedotov, V. Yu. Shishin, and V. A. Ovchinnikov, "Particulars of The Behavior under Irradiation of Dispersion Fuel Elements with Uranium Dioxide + Aluminium Alloy Fuel Composition", *Atomic Energy*, Vol.117, no. 4, pp. 251-256, 2015.
- [10] S. M. Dmitriev, A. A. Dobrov, M. A. Legchanov, and A. E. Khrobostov, "Modeling of Coolant Flow in The Fuel Assembly of the Reactor of A Floating Nuclear Power Plant Using The LOGOS CFD Program", *Journal of Engineering Physics and Thermophysics*, Vol. 88, no. 5, pp. 1297-1303, 2015.
- [11] S. M. Dmitriev, D. V. Doronkov, M. A. Legchaniv, A. N. Pronin, D. N. Solncev, V. D. Sorokin, and A. E. Hrobostov, "Investigating Hydrodynamic Characteristic and Peculiarities of the Coolant Flow Behind a Spacer Grid of a Fuel Rod Assembly of Floating Nuclear Power Unit", *Thermophysics and Aeromechanics*, Vol. 23, no. 3, pp. 369-378, 2016.
- [12] D. F. Baybakov, A. V. Godovykh, I. S. Martynov, "The dependence of the nuclide composition of the fuel core loading on multiplying and breeding properties of the KLT-40S nuclear facility", *Nuclear Energy and Technology*, vol. 2, pp. 183-190, 2016.
- [13] W. M. Stacey, *Nuclear Reactor Physics*, WILEY-VCH, Weinheim, 2007